

## Chapter 2

# Thermostatistics of small systems

At the thermodynamical limit, a first (second) order phase transition at say  $x = x_0 = \frac{\partial S}{\partial X}|_{X_0}$  is signaled by a singularity in the second (third) derivative of the free energy  $F$  (canonical potential) with respect to the intensive variables  $x$  [LY52A, LY52B, GR69, GL69]. From the properties of the probability distribution of the “extensive” variables  $X$  in CE (whenever  $F$  is singular or not), one can infer a definition of phases and phase transitions based on the *local* curvature of the microcanonical entropy-surface (see for systems depending on  $\mathcal{M} = 1$  “extensive” parameter [GM87, GMS97, GRO90, GRO01], special cases of  $\mathcal{M} = 2$  [GEZ96, GV00, GRO01] and a straightforward generalization in [FG01]).

In this chapter, these definitions and their origins are recalled and illustrated with the analytical models presented in section 1.4 on page 12. Some consequences of these new definitions and their link to the standard ones are also discussed. Finally, alternative definitions are reviewed and commented in section 2.5.

### 2.1 Pure phases

#### 2.1.1 Definition

At the thermodynamical limit a system is in a pure phase at say  $x_0$  when  $F$  is an infinitely differentiable function of  $x$  at  $x_0$  [LY52A, CAL85, GL69]. In a pure phase ME and CE are equivalent. The distribution of  $\frac{X}{N}$  in CE is a delta peak centered at  $X_0$ , where  $X_0$  satisfies  $x_0 = \frac{\partial S}{\partial X}|_{X_0}$ . For a finite system, the precursor of this delta peak is a distribution with a *maximum* at  $X_0$  (see sec. 1.2.2). This means that, at  $X_0$ , the entropy is a *concave* function. I.e.  $\lambda_1$ , the largest eigenvalue of the Hessian matrix of  $S$ , is negative. Thus, for a one dimensional system, its heat capacity is positive,  $C_V \propto - \left( \frac{\partial^2 S}{\partial X^2} \right)^{-1} > 0$ .

**Definition 3.** A microcanonical ensemble of states is in a pure phase at  $X = X_0$  if  $\lambda_1(X_0) < 0$ .

#### 2.1.2 Example

In fig. 2.1 on the next page the sign of  $\lambda_1$ , the largest eigenvalue of the Hessian matrix of  $s$  the entropy of the van der Waals model <sup>a</sup> (presented in section 1.2.1) is plotted versus the

---

<sup>a</sup> $s(\epsilon, v) \doteq \ln(v-1) + \frac{3}{2} \ln(\epsilon + \frac{1}{v})$ .

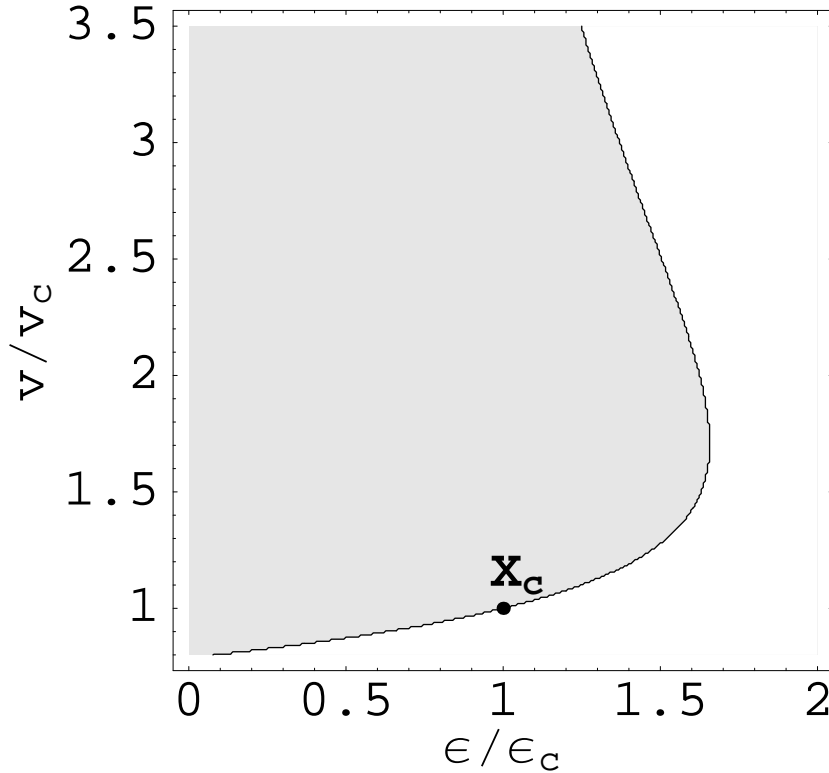


Figure 2.1: Sign of  $\lambda_1$ , the largest eigenvalue of the Hessian matrix of  $s$  for the van der Waals entropy-model. The white region at large volume corresponds to  $\lambda_1 < 0$  (pure phase). The gray region corresponds to  $\lambda_1 > 0$ .  $\lambda_1$  is equal to zero along the boarder-line between these two regions. The black dot locates the critical point  $X_c$  known from standard thermostatistics.

specific energy  $\epsilon$  and volume  $v$ . The white region at large energies corresponds to  $\lambda_1 < 0$  and therefore, according to def. 3, to a pure phase.

If one chooses a pressure  $p_0$  and a temperature  $T_0 = \beta_0^{-1}$  at say  $X_0 = (\epsilon_0, v_0)$ , i.e.  $\beta_0 = \frac{\partial s}{\partial \epsilon}|_{X_0}$  and  $\beta_0 p_0 = \frac{\partial s}{\partial v}|_{X_0}$  where  $\lambda_1(X_0) < 0$ , then  $f(X, X_0) = f(X, x_0 = (\beta_0, p_0)) = -x_0 \cdot X + s(X)$  has a local maximum at  $X_0$ . This is illustrated in fig. 2.2 on the facing page, where a density-contour plot of  $f$  is shown for  $(\epsilon_0, v_0) = (5, 5) \Rightarrow (\beta_0, p_0) = (\frac{5}{7}, \frac{17}{25}) \approx (0.71, 0.68)$ .  $f$  has a clear maximum at  $(5, 5)$ . It is even a *global* maximum. In this example, CE and ME are equivalent at  $X_0$  in the sense given in sec. 1.2.3.

## 2.2 First order phase transitions

### 2.2.1 Definitions

Pure phases are locally defined by a negative  $\lambda_1$ . What does happen to the probability distribution  $P(X, X_0)$  if  $\lambda_1(X_0) > 0$ ? First of all, for  $\mathcal{M} = 1$  (i.e.  $S(X) = S(E)$ ) this implies a *negative* specific heat capacity. There ME and CE cannot be equivalent. Furthermore, the probability distribution  $P(X, X_0) \propto \exp(f(X, X_0))$  has a *local minimum* at  $X_0$ .

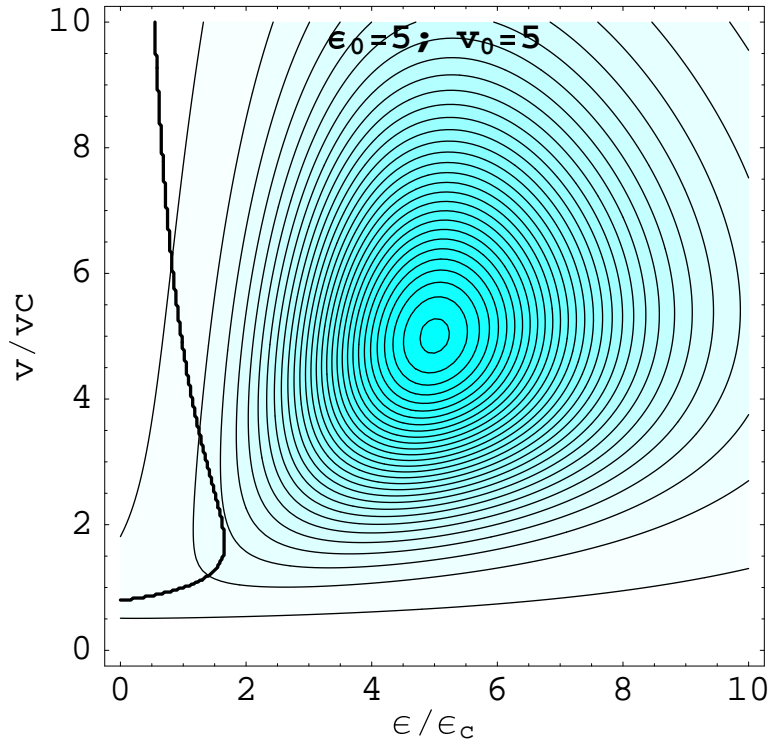


Figure 2.2: Contour-Density plot of  $f(X, X_0) \equiv f(X, x_0) = -x_0 \cdot X + s(X)$  for the van der Waals entropy-model at  $X_0 = (\epsilon_0, v_0) = (5, 5)$ , where  $x_0 = (\beta_0, \beta_0 p_0) = \frac{\partial s}{\partial X}|_{X_0} = (\frac{5}{7}, \frac{17}{35})$  and  $\lambda_1(X_0) < 0$ . There is a clear maximum at  $(\epsilon_0, v_0)$ . The gray level correspond to the value of  $f$ : the grayer the larger is  $f$ . The thick line corresponds to  $\lambda_1 = 0$  (see fig. 2.1 on the facing page); on the right side of this line  $\lambda_1 < 0$  and on the left one  $\lambda_1 > 0$ . The scale of  $f$  is non-linear.

This is illustrated in fig. 2.3(a) on the next page, where  $P(\epsilon, \epsilon_0)$  (unnormalized) is plotted for the entropy-model  $s_1^b$  for different value of  $\beta$ . The first one has been taken at  $\epsilon_0 = 0$  and the other at  $\epsilon_0 = 0.2$  which correspond to  $\beta = \beta_t = 1$  and  $\beta \approx 1.002$ , resp., and for  $N = 10^2$ . The two probability distributions have a minimum at their respective  $\epsilon_0$ . Moreover, in each distribution there are two maxima which have, by construction, the same temperature than their respective  $\epsilon_0$ , but their respective heat capacities are positive. I.e. the two peaks correspond to two pure phases. For  $\beta = 1$  the two peaks are of equal height, while for  $\beta = 1.002$  the peak at low energy is higher than the other one. In CE (at finite size and at  $\beta = \beta_t$ ), the two pure phases have the same probability of occurrence. Therefore, the fluctuations and consequently the specific heat capacity are large in CE (eq. (1.13) on page 8). Hence, the equivalence condition (2')<sup>c</sup> does not hold, although condition (1')<sup>d</sup> is fulfilled since  $\langle \epsilon \rangle_{CE} = \epsilon_0$  ( $f$  is an even function for  $\beta = \beta_t$ ). For  $\beta = 1.002$  the condition (1') clearly does not hold.

In fig. 2.3(b) the same distribution functions as in fig. 2.3(a) are plotted but this time for  $N = 10^3$ . The width of the peaks are smaller. For  $\beta = 1.002$  the smallest peak is of

<sup>b</sup> $s_1(\epsilon) \doteq \epsilon - 0.04(|\epsilon| - 0.5)^4 \theta(|\epsilon| - 0.5) - 0.01N^{-1/3} \cos(\pi\epsilon)$ , as defined in sec. 1.4.1.

<sup>c</sup>Small fluctuations of the “extensive” parameters in CE, see page 11.

<sup>d</sup> $\langle X \rangle_{CE} = X_0 = 0$ , see page 11.

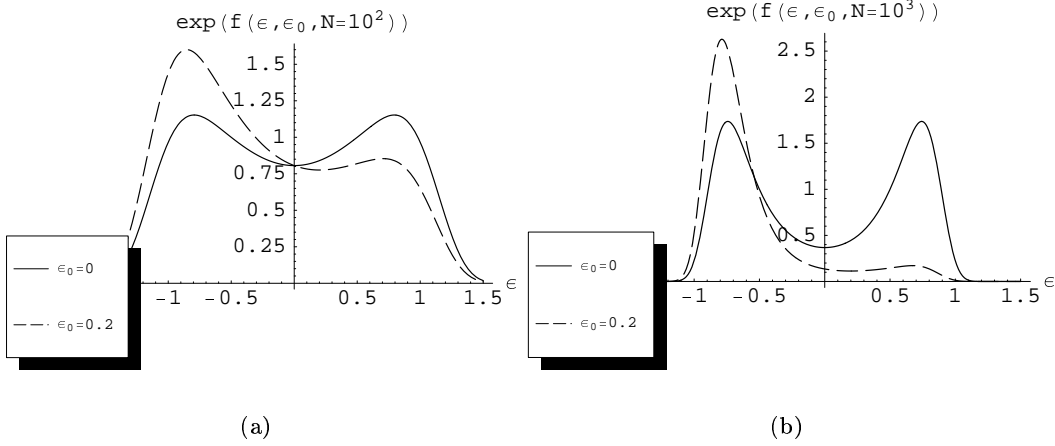


Figure 2.3: Unnormalized distribution functions  $P(\epsilon, \epsilon_0) \propto \exp(f(\epsilon, \epsilon_0)) = \exp\left(-\frac{\partial s_1}{\partial \epsilon}|_{\epsilon_0} \cdot \epsilon + s_1(\epsilon)\right)$  for the entropy model  $s_1$  (see eq. (1.20) or footnote (b) on the preceding page); for two values of  $N$  and of temperatures  $T_0^{-1} = \frac{\partial s_1}{\partial \epsilon}|_{\epsilon_0}$ . When  $\epsilon_0$  is chosen in the region of negative specific heat capacity, the probability distribution of  $\epsilon$  has a double peak structure.

no importance compared to the one at low energy. At the thermodynamical limit, this distribution function is simply a single Dirac distribution at  $\epsilon \approx -0.8$ , and not at  $\epsilon = \epsilon_0!$  Now, for  $\beta = 1$ , i.e.  $\epsilon_0 = 0$ , the two peaks remain. At the thermodynamical limit, the distribution function is composed of *two* delta Dirac<sup>e</sup>, one at  $\epsilon = -0.5$  and the other at  $\epsilon = 0.5$ . In CE, the fluctuations of the energy are larger for  $\beta = 1$  and smaller for  $\beta = 1.002$ . But nevertheless, the equivalence conditions (1') or (2') do not hold for any of the two  $\epsilon_0$ .

These two delta peaks are at the origin of the critical behavior of  $F$  at a first order phase transitions [GRO97]. Consider the system at the thermodynamical limit and its probability distribution for  $X$ , i.e.  $\lim_{N \rightarrow \infty} P\left(\frac{X}{N}, \frac{X_0}{N}\right)$ . At  $\beta = \beta_t - \delta\beta \lesssim \beta_t$ ,  $P$  has a single peak at  $\frac{X_0}{N} \equiv \epsilon_0 = \langle \epsilon \rangle_{CE} \lesssim -0.5$ . At  $\beta = \beta_t + \delta\beta \gtrsim \beta_t$ ,  $P$  has a single peak at  $\frac{X_0}{N} \equiv \epsilon_0 = \langle \epsilon \rangle_{CE} \gtrsim 0.5$  and at exactly  $\beta = \beta_t$ ,  $P$  has *two* peaks, one at  $\epsilon_1 = -0.5$  and the other at  $\epsilon_2 = 0.5$  (implying  $\langle \epsilon \rangle_{CE} = (\epsilon_1 + \epsilon_2)/2$ ). Consequently, in CE,  $\beta$  is a *discontinuous* function of  $\langle \epsilon \rangle$ . Therefore, the specific heat capacity  $C_V = \frac{\partial \langle \epsilon \rangle}{\partial \beta^{-1}}$  *diverges* at  $\beta = \beta_t$ . This divergence signals a first order phase transition in standard

<sup>e</sup>It may be not clear why  $P$  should be composed of two peaks at the thermodynamical limit and at the transition temperature. Indeed, at the limit  $N \rightarrow \infty$ ,  $s_1 \doteq s_\infty + N^{-1/3} s_{surf}$  is just  $s_\infty \doteq \epsilon - 0.04(|\epsilon| - 0.5)^4 \theta(|\epsilon| - 0.5)$ .  $s_\infty$  is a linear function of  $\epsilon$  in the range  $[-0.5, 0.5]$ . Therefore  $P$  should be simply flat in this interval.

This argument is not correct since the limit  $N \rightarrow \infty$  has been taken too soon. Consider  $P(\epsilon, N) \propto \exp\left(N\left(-\epsilon\beta + s_\infty(\epsilon) + N^{-1/3} s_{surf}(\epsilon)\right)\right)$  for a finite  $N$ , at the transition temperature  $\beta = \beta_t$  and for  $\epsilon \in [-0.5, 0.5]$ . The points in the transition region are suppressed exponentially because  $N(s_\infty - s_1) = N^{2/3} S_{surf} < 0$ . When  $N \rightarrow \infty$ , although the *relative* weight of  $S_1$  compared to  $S_\infty$  vanishes, i.e.  $\lim_{N \rightarrow \infty} \frac{S_1}{S_\infty} = \lim_{N \rightarrow \infty} \frac{s_\infty + N^{-1/3} s_{surf}}{s_\infty} = 1$ , their *absolute* difference *diverges*  $\lim_{N \rightarrow \infty} S_\infty - S_1 = \lim_{N \rightarrow \infty} N^{2/3} s_{surf} = -\infty$ , leading to the double  $\delta$ -peak shape of  $P$  at the limit  $N \rightarrow \infty$ . This illustrates nicely the danger of taking the limit  $N \rightarrow \infty$  too soon.

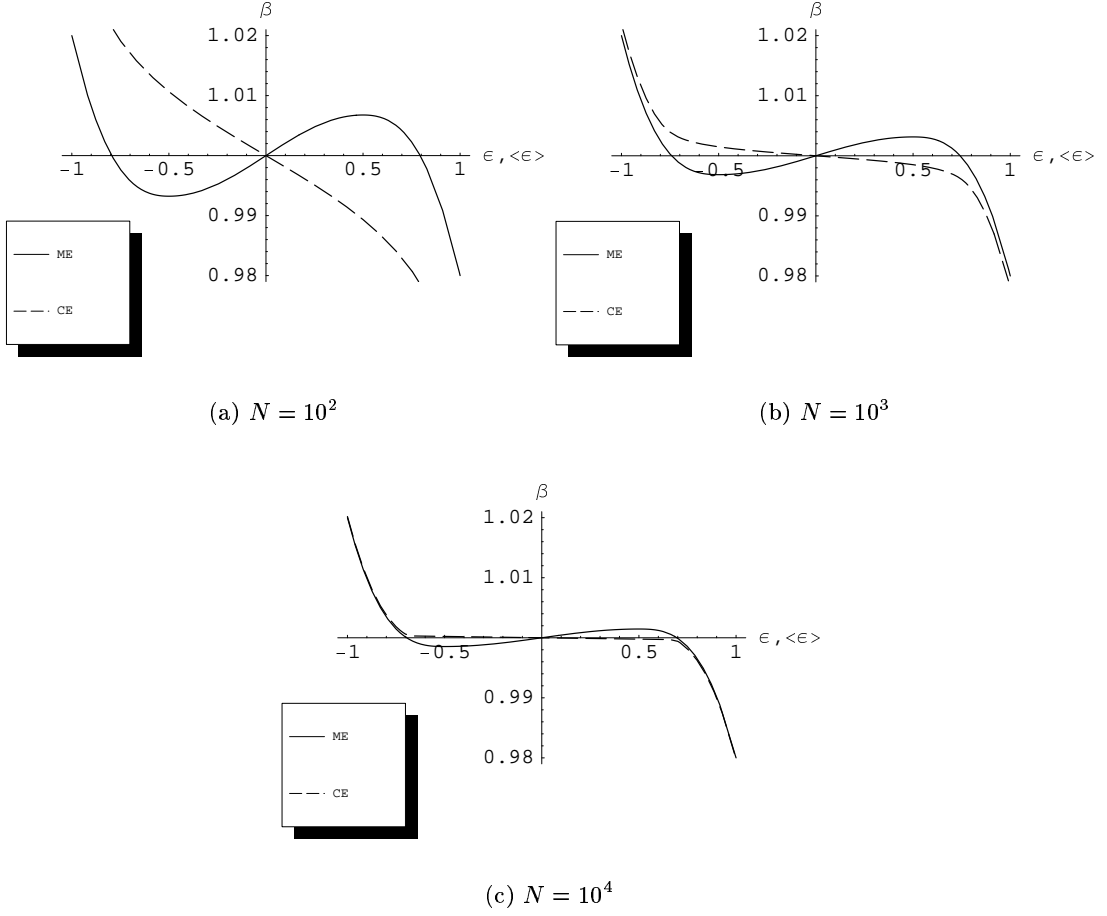


Figure 2.4: Inverse temperature as a function of  $\epsilon$  (ME; plain lines),  $\langle \epsilon \rangle$  (CE; dashed lines) and  $N$  for the model  $s_1$  (see eq. (1.20) or footnote (b) on page 19).  $\beta_{ME}(\epsilon, N) \doteq \frac{\partial s_1}{\partial \epsilon} = -0.16(|\epsilon| - 0.5)^3 + 0.01\pi N^{-1/3} \sin(\pi\epsilon)$ . For finite  $N$ ,  $\frac{\partial \beta_{ME}}{\partial \epsilon} > 0$  for  $\epsilon \in ]-0.5, 0.5[$ , whereas  $\frac{\partial \beta_{CE}}{\partial \langle \epsilon \rangle} < 0$  for any  $\langle \epsilon \rangle$ . With increasing  $N$  the differences between both inverse temperatures vanish. However, in the limit  $N \rightarrow +\infty$ ,  $\beta_{CE}$  is not defined for  $\langle \epsilon \rangle \in ]-0.5, 0[ \cup ]0, 0.5[$  in contrast to  $\beta_{ME}$  which is defined for all  $\epsilon$ . The discontinuity of  $\langle \epsilon \rangle$  ( $\beta_{CE}$ ) leads to the conventional signal of a first order phase transition.

thermostatistics [RUE69, CAL85, LL94, LY52A].

In fig. 2.4 the inverse temperature curves for the same entropy-model  $s_1$  are plotted versus  $\epsilon$  (microcanonical  $\beta \equiv \beta_{ME}$ ) and  $\langle \epsilon \rangle$  (canonical  $\beta \equiv \beta_{CE}$ ) for different  $N$ . For all  $N$ ,  $\beta_{ME}$  and  $\beta_{CE}$  are clearly different in the energy range  $[-0.5, 0.5]$  where the microcanonical specific heat capacity is negative. Close to these regions even though  $\lambda_1 < 0$ , ME and CE are also not equivalent because of the presence of a second peak in their respective canonical distribution functions (see fig. 2.3). For small systems, a phase transition in ME implies the non-equivalence between the ensemble, while the non-equivalence does not lead to a phase transition (in ME). With increasing  $N$ , these non-equivalence regions with  $\lambda_1 < 0$  shrinks to the transition region if the surface effects vanishes. For increasing  $N$ , both the microcanonical and the canonical specific heat capacity increases at  $\beta = \beta_t$  to

eventually diverge at the limit  $N \rightarrow \infty$ . Again, this signals a first order phase transition.

The previous examples enlighten the fact that the singularity signaling a first order phases transition at the thermodynamical limit has its origins in an anomalous curvature of  $S$ , i.e.  $\lambda_1 > 0$ . The converse statement is not necessarily true, i.e. a negative curvature at a given finite  $N$  does not imply a phase transition at the limit  $N \rightarrow \infty$ , indeed nothing forbids the sign of  $\lambda_1$  to be also a function of  $N$  at fixed  $\frac{X_0}{N}$ .

**Definition 4.** *A microcanonical ensemble of states is in a first order phase transition at  $X = X_0$  if  $\lambda_1(X_0) > 0$ .*

The eigenvalue  $\mathbf{v}_1$  associated with  $\lambda_1$  gives the direction of the largest negative curvature. In simple models when one follows the trajectory given by  $\mathbf{v}_1$ <sup>f</sup>, one reaches the two extrema (pure phases) which have the same  $x_0$  than the one at  $X_0$ . Therefore,  $\mathbf{v}_1$  gives the direction of the *local order parameter* (see below and also [GRO01]).

**Definition 5.** *The direction of the local order parameter of a first order phase transition is given by  $\mathbf{v}_1$ .*

Note that, for a multidimensional  $X$ , there might be many positive eigenvalues (say from  $i = 1, \dots, k$ ), this means that there are several first order phase transitions. A basis for the order parameters is simply given by the set  $\{\mathbf{v}_1, \dots, \mathbf{v}_k\}$ .

There is an important point to add. From the fig. 2.3 on page 20 one sees that the information contained in the region where  $\lambda_1 > 0$  are overridden by the ones coming from the dominant peak (see also footnote (e) on page 20). Information contained in the convex part of  $S$  is smeared out in CE [HÜL94A]. Formally no information is lost since one can always perform a inverse Laplace transform (when of course the equivalence condition (0)<sup>g</sup> is fulfilled). But this inverse transform is in practice so unstable that this information is actually *lost* in CE [CH88].

So far, only models with simple topological entropy-surfaces have been studied. For these models a first order transition region always led to two local maxima in  $f$  connected by the curve of constant control parameter (as defined in footnote (f)). However, a priori, more complicated cases (i.e. with more than two maxima) are not excluded (see for a “three-peaks” system [GRO01]).

### 2.2.2 Example

In fig. 2.5 on the facing page,  $\exp \left\{ f(X, X_0) \right\} \propto P(X, X_0)$  is plotted for the van der Waals entropy-model.  $X_0 = (\epsilon_0, v_0) = (0.94, 1)$  has been chosen in the region where  $\lambda_1 > 0$ . At  $(\epsilon_0, v_0)$ ,  $f$  has a saddle point because the second eigenvector  $\lambda_2$  is negative. One sees also, just like for the one dimensional model in fig. 2.3, that  $f$  has two maxima in the pure phase region. One corresponds to the liquid phase (small  $\epsilon$  and  $v$ ) and the other to the gas phase. By construction, their temperature and pressure are the same than the ones at  $X_0$ .

The fig. 2.6 on page 24 is the same as fig. 2.5 plus the vector field  $\mathbf{v}_1$ , and the line of constant control parameter that goes through  $X_0 = (\epsilon_0, v_0)$  as defined in footnote (f). It

<sup>f</sup>It is the line solution of the following differential equation

$$\dot{X}(t) = \mathbf{v}_1(X(t)), \tag{2.1}$$

with  $X(t=0) = X_0$  and  $t \in ]-\infty, +\infty[$  is a parameter. This line can be labeled by a *control parameter*.

<sup>g</sup>Finite partition function, see page 11.

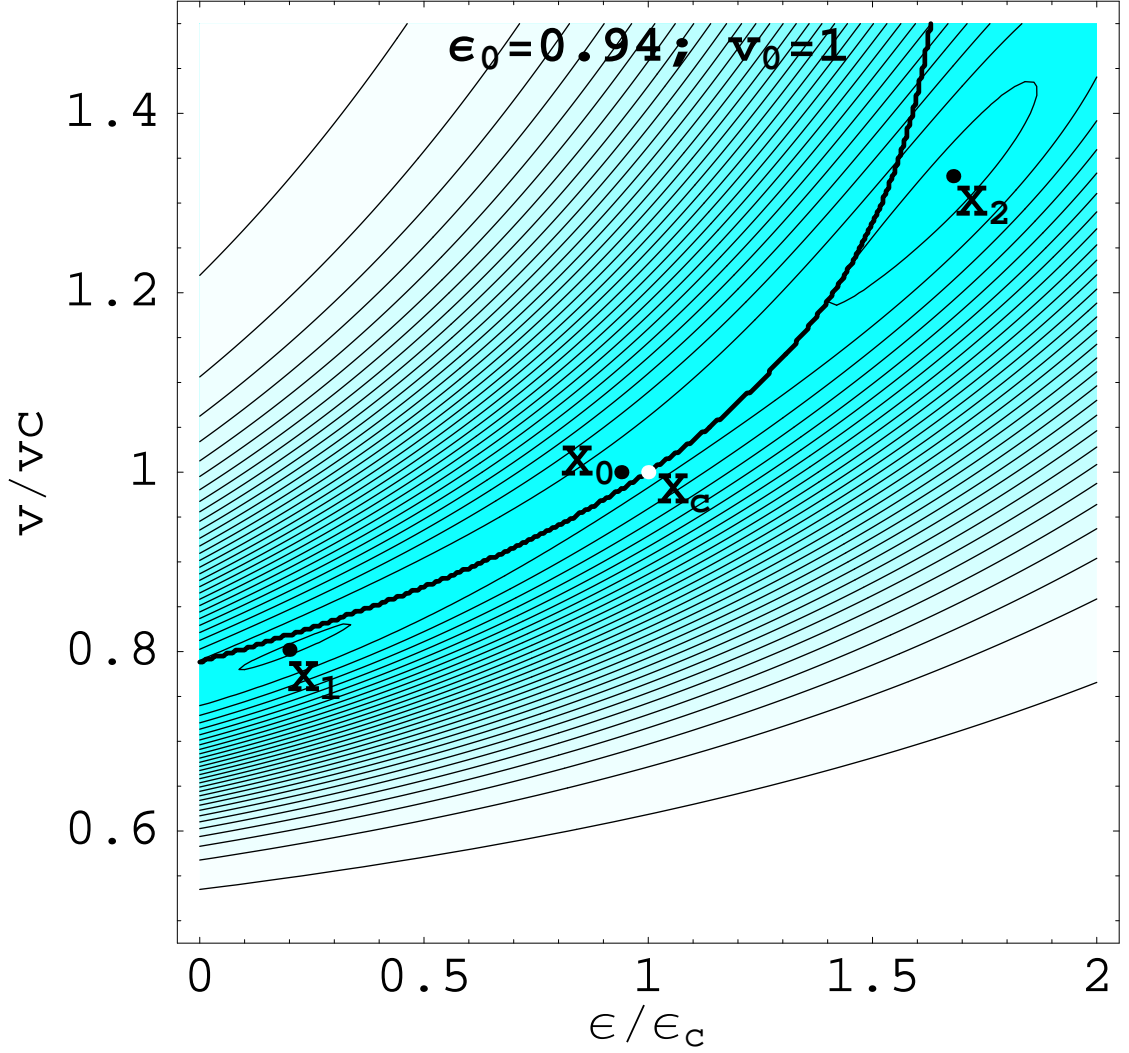


Figure 2.5: Contour-Density plot of  $f(X, X_0) = -x_0 \cdot X + s(X)$  for the van der Waals entropy-model at  $X_0 = (\epsilon_0, v_0) = (0.94, 1)$ , where  $x_0 = \frac{\partial s}{\partial X}|_{X_0}$ . The thick line corresponds to  $\lambda_1 = 0$ . Below (above) it,  $\lambda_1$  is negative (positive), hence  $\lambda_1(X_0) > 0$ .  $f$  has two local maxima one at  $X_1 \approx (1.68, 1.32)$  and another at  $X_2 \approx (0.2, 0.8)$  which correspond to two pure phases peak ( $\lambda_1(X_{1,2}) < 0$ ).  $f$  has a saddle point at  $X_0 = (\epsilon_0, v_0)$  ( $\lambda_1(X_0) > 0$  and  $\lambda_2(X_0) < 0$ ). By construction,  $\frac{\partial s}{\partial X}|_{X_1} = \frac{\partial s}{\partial X}|_{X_2} = \frac{\partial s}{\partial X}|_{X_0} = x_0$ . In CE the main contributions to the partition function  $\mathcal{Z}(x_0)$  comes from the two peaks  $X_1$  and  $X_2$ , and the information from  $X_0$  is in practice lost. The white dot locates the critical point  $X_c$ .

nicely illustrates the definitions of the order and control parameters. If one follows the curve tangent to  $\mathbf{v}_1$  starting from  $X_0$  (gray line in fig. 2.6), one eventually reaches the gas or liquid extrema (labeled by  $X_1$  and  $X_2$ ). Along this gray line  $f$  has an extremum<sup>h</sup> in the  $\mathbf{v}_2$  direction, in a symbolic formulation

$$\nabla f \cdot \mathbf{v}_1 = 0. \quad (2.2)$$

<sup>h</sup>Here it is an maximum since  $\lambda_2 < 0$ .

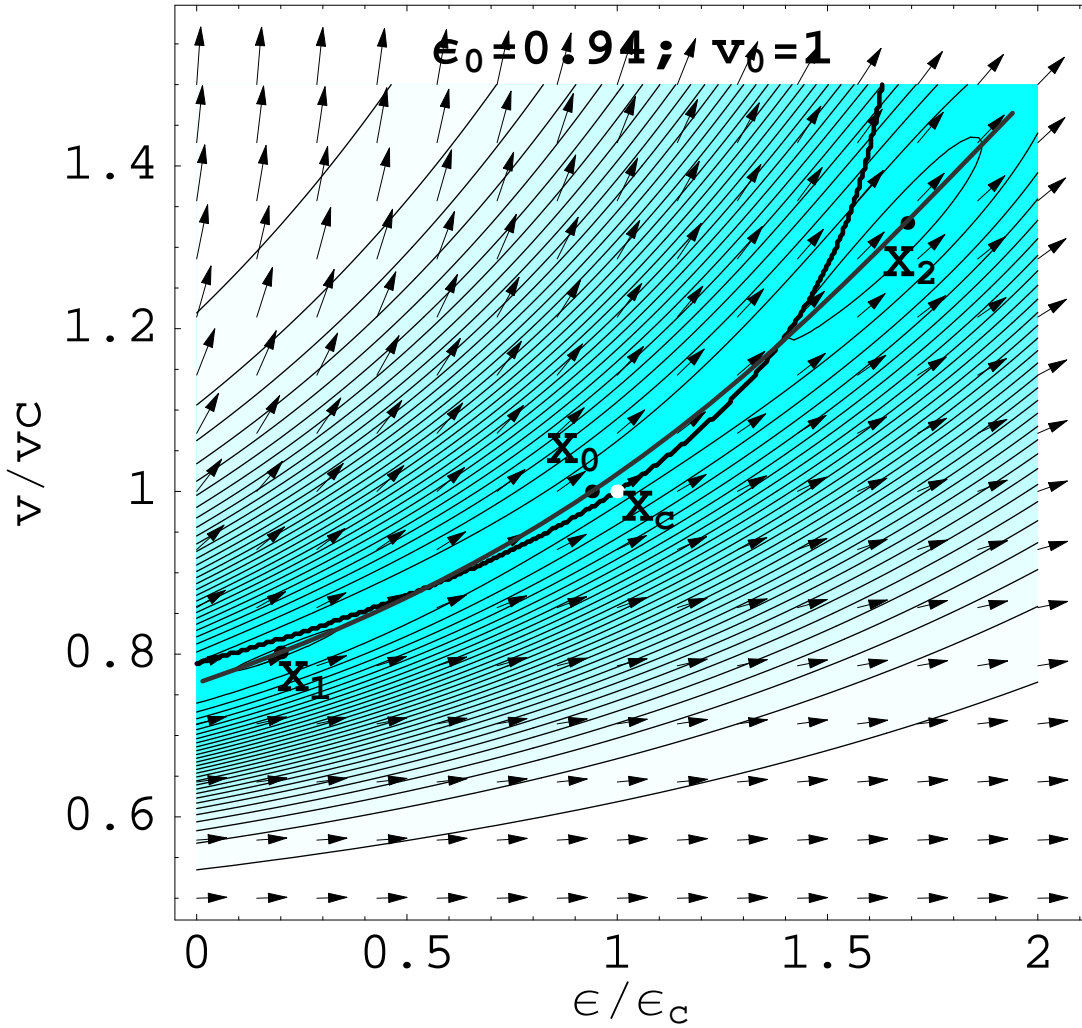


Figure 2.6: Contour-Density plot of  $f(X, X_0) = -x_0 \cdot X + s(X)$  for the vdW entropy-model at  $X_0 = (\epsilon_0, v_0) = (0.94, 1)$ , where  $x_0 = \frac{\partial s}{\partial X}|_{X_0}$ , plus the vector field  $\mathbf{v}_1$  and the line of constant control parameter (as defined in footnote (f) on page 22) that goes through  $X_0$  (gray line; see fig. 2.7). As one can see this line goes also through the two maxima  $X_1$  and  $X_2$ . At the maxima, by construction the values of the inverse temperature and pressure are equal to  $x_0$  (which are defined at  $X_0$ ). The thick line corresponds to  $\lambda_1 = 0$ , below (above) it  $\lambda_1$  is negative (positive). The critical point  $X_c$  is located by a white dot.

In fig. 2.7 on the next page, the parametric lines  $(\epsilon(t), \alpha_\beta(t))$  and  $(\epsilon(t), \alpha_p(t))$  along the constant control parameter line in fig. 2.6 are shown, where

$$\alpha_\beta(t) \doteq \frac{|\beta(t) - \beta(X_0)|}{\beta(X_0)}, \quad (2.3)$$

$$\alpha_p(t) \doteq \frac{|p(t) - p(X_0)|}{p(X_0)}, \quad (2.4)$$

and  $t$  is the “time” parameter as defined in footnote (f) on page 22. This figure shows that the gray line goes indeed through the two local maxima in the pure phase regions.



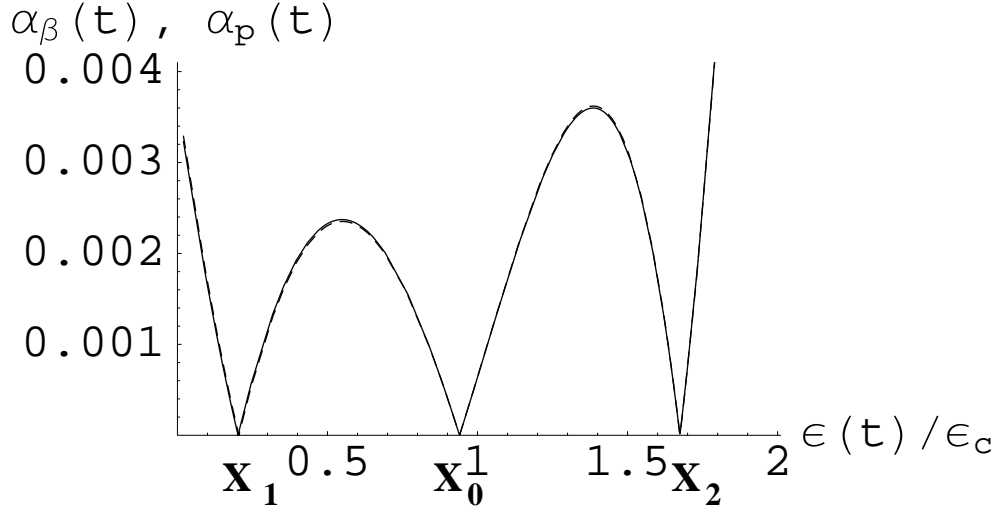


Figure 2.7: Parametric plots  $(\epsilon(t), \alpha_\beta(t))$  (dashed line) and  $(\epsilon(t), \alpha_p(t))$  (plain line) along the constant control parameter line (as defined in footnote (f) on page 22) with  $X_0 = (\epsilon_0, v_0) = (0.94, 1)$  (gray line in fig. 2.6).  $\alpha_\beta$  and  $\alpha_p$  are the relative difference between resp.  $\beta_0$  and  $p_0$  as a function of  $t$  where  $(\beta_0, \beta_0 p_0) = x_0 = \frac{\partial S}{\partial X}|_{X_0}$  (see eqs. (2.3) and (2.4)).  $\alpha_p(t) = \alpha_\beta(t) = 0$ , for  $t$  such that  $X(t)$  is equal to  $X_0, X_1$  or  $X_2$ .

The two equations  $\alpha_\beta(t) = 0$  and  $\alpha_p(t) = 0$  shares the same three solutions,  $t_0, t_1$  and  $t_2$  which correspond time to  $X(t_i) = X_i, i = 0, 1$  and  $2$ .

In fig. 2.8 on the following page, the vector field  $\mathbf{v}_1$  for the van der Waals model is plotted along with the sign of  $\lambda_1$  and with the contour plots of the inverse temperature  $\beta$  and of  $\beta p$ . I.e.  $\beta$  and  $\beta p$  are constants along their respective contour lines. The lines  $\beta p = cst$  are almost <sup>i</sup> tangent to  $\mathbf{v}_1$ . Hence,  $\beta p$  is at a good approximation a control parameter.

Although it is hardly to be seen on fig. 2.8, due to the scale and to the orientation of the axes, the lines of constant  $\beta$  and the one of constant  $\beta p$  cross each other one or three times (as checked in fig. 2.7). In the latter case one crossing is located in the  $\lambda_1 > 0$  region.

Another point worth to be noticed, is that at  $\lambda_1 = 0$ , the lines of constant  $\beta$  and constant  $\beta p$  are parallel to each other and also to  $\mathbf{v}_1$ , i.e.

$$\nabla\beta \wedge \nabla\beta p = 0, \quad (2.5a)$$

and

$$\nabla\beta \cdot \mathbf{v}_1 = 0. \quad (2.5b)$$

This is easy to understand since

$$\nabla\beta = \nabla \left( \frac{\partial s}{\partial \epsilon} \right) = \left( \begin{array}{c} \frac{\partial^2 s}{\partial \epsilon^2} \\ \frac{\partial^2 s}{\partial v \partial \epsilon} \end{array} \right) \quad (2.6a)$$

<sup>i</sup>The angle  $\theta$  between  $\mathbf{v}_1$  and  $\nabla\beta p$  is  $\pi/2$  along the line  $\lambda_1 = 0$ , elsewhere in the parametric range used on fig. 2.8 the absolute difference  $|\theta - \pi/2|$  is of the order of  $10^{-9}$ .

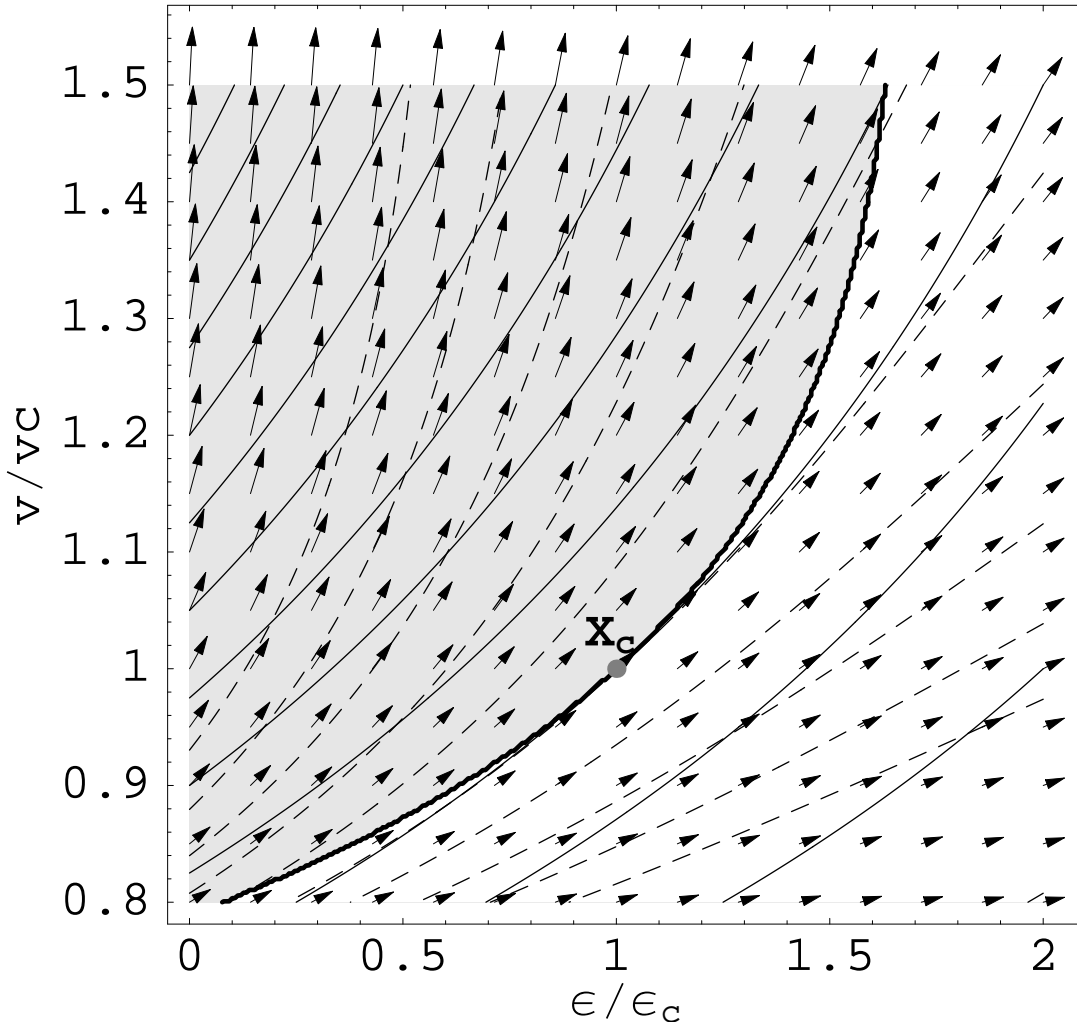


Figure 2.8: vdW entropy-model. Vector field  $\mathbf{v}_1$ ; Contour-plot  $\beta = cst$  and  $\beta p = cst$  solid and dashed lines, respectively. Sign of  $\lambda_1$ : gray shaded region  $\lambda_1 > 0$  (first order phase transition), white region  $\lambda_1 < 0$  (pure phase). The dot at  $(\epsilon, v) = (1, 1)$  locates the critical point of the first order phase transition of the vdW entropy-model. The vectors  $\mathbf{v}_1$  are almost tangent to the lines  $\beta p = cst$ , i.e. at a good approximation  $\beta p$  is the control parameter of this first order phase transition.

and

$$\nabla\beta p = \nabla \left( \frac{\partial s}{\partial v} \right) = \begin{pmatrix} \frac{\partial^2 s}{\partial \epsilon \partial v} \\ \frac{\partial^2 s}{\partial v^2} \end{pmatrix} \quad (2.6b)$$

which are the columns of  $H_S$ , the Hessian matrix of  $S$  in the coordinates  $(\epsilon, v)$ . Now, the fact that  $\lambda_1 = 0$  implies that these columns are linear combinations of the eigenvectors whose eigenvalues are not zero. Thus, the columns are linearly dependent. Therefore, and as the dimension of the parametric space is two,  $\nabla\beta \propto \nabla\beta p \propto \mathbf{v}_2 \perp \mathbf{v}_1$ . The latter relations lead to eqs. 2.5a. In other words, at  $\lambda_1 = 0$  the constant intensive parameters lines are all parallel to each other and to  $\mathbf{v}_1$ .

In fig. 2.8 one can also notice that the lines of constant intensive parameters are tangent to the line  $\lambda_1 = 0$  at the critical point  $X_c$ . This is discussed further in sec. 2.3.

The eqs. (2.5) can trivially be extended for  $\mathcal{M} > 2$ . The gradients of  $x = \{x_1, \dots, x_{\mathcal{M}}\}$  are linear combinations of the eigenvectors whose eigenvalues are non null. Therefore, if e.g.  $\lambda_1 = 0$  then  $\{\nabla x_1, \dots, \nabla x_{\mathcal{M}}\}$  is a set of linearly dependant vectors which are all orthogonal to  $\mathbf{v}_1$ .

### 2.2.3 Transition parameters

In classical thermodynamics one characterizes first order phase transitions by some couples of quantities, the transition parameters, e.g. transition temperature  $T_t \doteq \frac{1}{\beta_t}$ , latent heat  $q_{lat}$ , surface tension  $\gamma$ , etc.

These parameters are well defined for infinite systems. However, for small ones they hardly make sense. As one can see on figs. 2.4 on page 21, there is no temperature at which the transition take place, but on the contrary, the transition occurs (in ME sense) within a certain *range* of temperatures. Of course, at the thermodynamical limit, if it exists, this range shrinks to one point and the usual definition of the transition temperature is recovered. As the other transition parameters rely on the value of  $T_t$ , they are in their turn not unambiguously defined for small systems. For the surface tension  $\gamma$ , the difficulties are even greater since it is almost impossible to define surface areas for small systems. Indeed, in macroscopic systems the interphase is a two dimensional object only at a first approximation. The density of the liquid does not abruptly change from its liquid value to its vapor one; it decreases smoothly over a length of the order of the particle interaction range. Hence, for a small system, whose size is of the order of the interaction range, the definition surfaces are rarely unambiguous (an exception is e.g. spin systems [GEZ96]). E.g. for the liquid–gas transition of metallic clusters how to define a gas part, a liquid part, and a surface area between them when the system is composed of a few thousands of atoms?

Again all these parameters are defined in the limit  $N \rightarrow \infty$ . Nevertheless, it could be useful to have some “finite–size” definitions (though ambiguous and inaccurate) in order to make the bridge to their thermodynamical limit ones. I.e. definitions that converge to the usual ones at the limit  $N \rightarrow \infty$ . This can be useful to perform some finite–size scaling as done in sec. 3.4.

$\mathcal{M} = 1$

A convex intruder in the specific entropy curve  $s(\epsilon)$  is forbidden for infinite systems, because there the system gains entropy if it would divide itself into two pieces one with specific energy  $\epsilon = \epsilon_1$  and the other with  $\epsilon = \epsilon_3$  see fig. 2.9(a) on the next page. Both pieces together would have a larger entropy  $s_{hull}(\epsilon) = \alpha_1 s(\epsilon_1) + \alpha_3 s(\epsilon_3) \geq s(\epsilon = \alpha_1 \epsilon_1 + \alpha_3 \epsilon_3)$ , where  $\alpha_1 = \frac{\epsilon - \epsilon_3}{\epsilon_1 - \epsilon_3}$ ,  $\alpha_3 = \frac{\epsilon_1 - \epsilon}{\epsilon_1 - \epsilon_3}$  and  $\alpha_1 + \alpha_3 = 1$  are the relative sizes of the two parts<sup>j</sup> [CAL85, HÜL94B]. Then, the slope of  $s_{hull}$  gives the transition temperature  $\beta_t$ . An equivalent approach is to make the Maxwell construction (see fig. 2.9(b); there  $\beta_t = 1$ ). The latent heat  $q_{lat}$  is simply given by  $q_{lat} = \epsilon_3 - \epsilon_1$ , i.e. by the length of the Maxwell construction segment. By construction, in fig. 2.9(b) the shaded area on the left side below  $\beta_{tr}$  is equal to the one on the right side above  $\beta_t$  and also to  $s_{hull}(\epsilon_2) - s(\epsilon_2) \doteq \Delta s_{surf} \equiv \Delta s$  the surface entropy, see also fig. 2.9(a).

<sup>j</sup>It is implicitly assumed that the surface effects can be neglected [GRO01, GRO00B].

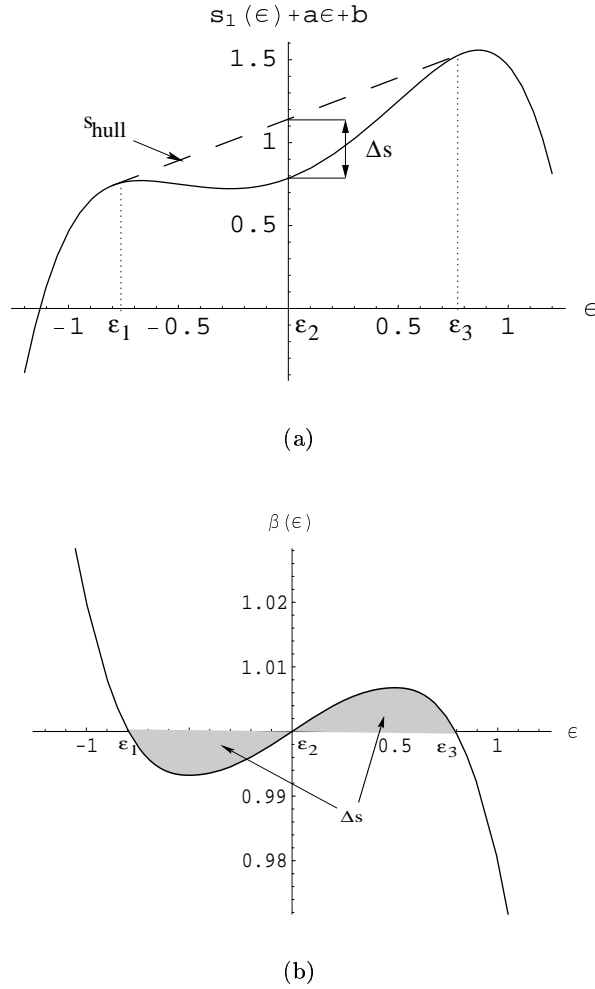


Figure 2.9: Determination of the transition parameters for the entropy-model  $s_1$  (as defined in sec. 1.4.1, eq. (1.20)),  $N = 100$ . At a first order phase transition, the specific entropy has a convex intruder (panel (a); for conveniency a linear function of  $\epsilon$  is added to  $s_1$ ,  $a = -0.5$ ,  $b = 1$ ). For short-range interaction systems, this intruder is forbidden by van Hove's theorem [vH49] in the limit  $N \rightarrow +\infty$ . Indeed, those systems would gain entropy by splitting up into two parts, one at specific energy  $\epsilon_1$  and the other at  $\epsilon_3$  (the resulting entropy is  $s_{hull}$  in panel (a)). For finite system,  $\frac{\partial s_{hull}}{\partial \epsilon} \doteq \beta_t$  defines the transition temperature  $T_t = \beta_t^{-1}$ . This temperature is also the one given by the Maxwell construction (panel (b)). The latent heat can be defined as  $\epsilon_3 - \epsilon_1$ , the length of the Maxwell segment, or alternatively, as  $0.5 - (-0.5) = 1$ , the length of the negative specific heat capacity region (see text). At  $\epsilon_2$ ,  $\Delta s = s_{hull} - s_1$ , the entropy-loss induced by the surface correlations is by construction equal to the areas between the Maxwell line and the lobes of the  $\beta$  curve (gray shaded areas in panel (b)).

The intra-phase surface  $\gamma$  tension is related to  $\Delta s_{surf}$  by

$$\gamma = \nabla s_{surf} T_t \frac{N}{\mathcal{A}}, \quad (2.7)$$

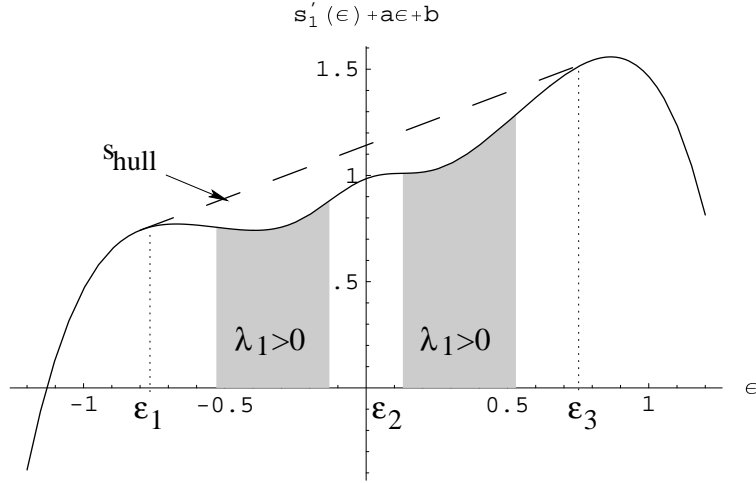


Figure 2.10: Specific entropy  $s'_1(\epsilon) = s_1(\epsilon) + \frac{1}{5} \exp(-20\epsilon^2)$  ( $a = -0.5$ ,  $b = 1$ ); for  $|\epsilon| \gtrsim 0.5$   $s'_1(\epsilon) \approx s_1(\epsilon)$ . If one uses the convex hull  $s_{hull}$  ( $\sim$  Maxwell line) to define first order phase transitions ( $\sim$  canonical definition), one would conclude that there is *one* first order phase transition between  $\epsilon_1$  and  $\epsilon_3$  (just like for  $s_1$ , see fig. 2.9(a)). However, in the microcanonical sense there are *two* phase transition regions for  $|\epsilon| \in ]0.13, 0.53[$  ( $\lambda_1(\epsilon) > 0$ ). This is an illustration of the deeper insight that gives ME compared to CE into small systems phase transitions. Moreover, it shows also how ambiguous can be the definition of transition parameters based on the Maxwell construction.

where  $\mathcal{A}$  is the surface area.

As an approximation, one can use these definitions for small systems with  $\mathcal{M} = 1$ . However, as already mentioned they are ambiguous and should be used with caution. As an example, one can realize that these definitions consider everything below the Maxwell line as being a mixture of two pure phases (the ones at the end points of this line). But a priori, there is no reason that forbids the presence of another pure phase below this line, i.e. a region characterized by  $\lambda_1 > 0$  but whose entropy is smaller than  $s_{hull}$  (see for an illustration fig. 2.10). In this sense, the surface entropy and the other usual macroscopic transition parameters are *global* properties of  $s$ , because at one point  $X = X_0$ ,  $\Delta s$  depends on the values taken by  $s$  on the *whole* parameter space.

An alternative definition for the latent heat is the length of the energy region over which the specific heat capacity is negative (in fig. 2.9 on the preceding page,  $q_{lat} = 0.5 - (-0.5) = 1 < \epsilon_3 - \epsilon_1$ ). At the thermodynamical limit, the two definitions for  $q_{lat}$  are equivalent.

$\mathcal{M} > 1$

For these systems there is so far no equivalent of the Maxwell construction. The simplest solution is to reduce the problem to a one dimensional one by considering only the lines at constant control parameter (gray line in fig. 2.6). This allows to have  $s$  as a function of a unique parameter order and to use the machinery developed for  $\mathcal{M} = 1$ .

Again, the parameters obtained are ambiguous and global. One should use them only to make the bridge to their infinite system values.

## 2.3 Second order phase transitions

### 2.3.1 Definition

At a second order phase transition the surface tension between the phases vanishes. Two (or more) phases coexist without any entropy loss. E.g. for  $\mathcal{M} = 1$  when the two peaks in  $P(E)$  at  $\beta_t$  are infinitely close from each other leading to macroscopic fluctuation of  $\epsilon$  in CE. But, in contrast with a first order phase transition,  $\langle \epsilon \rangle$  is still a continuous function of  $\beta$  at a critical point. In one dimension, these transitions are characterized by  $\frac{\partial \beta}{\partial \epsilon} = \frac{\partial^2 s}{\partial \epsilon^2} = 0$  and  $\frac{\partial^2 \beta}{\partial \epsilon^2} = \frac{\partial^3 s}{\partial \epsilon^3} = 0$ . Taking as an example the van der Waals entropy-model, one can see in fig. 2.11 how the two peaks merges when one approaches the critical point from the first order phase transition region. In a multidimensional parameter-space the above mentioned criteria for 1-D systems can be extended as: first  $\lambda_1 = 0$  and second  $\boldsymbol{\alpha} \cdot \nabla \lambda_1 = 0$ , where  $\nabla \lambda_1$  is the gradient of  $\lambda_1$  and  $\boldsymbol{\alpha}$  is a yet unknown vector that gives simply the direction along which  $\lambda_1$  is flat up to the first order approximation ( $\sim$ vanishing third derivative of  $S$ ). From the infinite systems and from the fact that often second order transitions are end-points of first order ones it can be inferred that this derivatives vanishes along the order parameter [LL94], i.e.  $\mathbf{v}_1$ . Hence, the second criteria is  $\mathbf{v}_1 \cdot \nabla \lambda_1 = 0$  [GV99, GRO01].

**Definition 6.** *A microcanonical ensemble of states is in a second order phase transition at  $X = X_0$  if  $\lambda_1(X_0) = 0$  and  $\mathbf{v}_1(X_0) \cdot \nabla \lambda_1(X_0) = 0$ .*

The first eigenvalue  $\lambda_1$  may not be the only one to fulfill the condition given in def. 6, i.e.  $\lambda_i(X_0) = 0$  and  $\mathbf{v}_i(X_0) \cdot \nabla \lambda_i(X_0) = 0$  for  $i = 1, \dots, k \leq \mathcal{M}$ , in this case  $X_0$  is called a *multicritical* point.

For a system depending on two “extensive” parameters ( $\mathcal{M} = 2$ ), it is shown in sec. 2.2.2 that, where  $\lambda_1 = 0$ , the lines of constant intensive parameters are parallel to each other and to  $\mathbf{v}_1$ . The second criterium in def. 6 implies that the line of constant intensive parameters are parallel to the line  $\lambda_1 = 0$  (as already notices in the previous section).

This equivalent condition for second order phase transition can also be straightforwardly generalized for  $\mathcal{M} > 2$ . At a critical point the lines of constant intensive parameters are orthogonal to  $\mathbf{v}_1$  where  $\lambda_1 = 0$ .

### 2.3.2 Example

Fig. 2.11(a)–(c) show how for the vdW entropy-model the two pure phases peaks merge when  $X_0 \rightarrow X_c$  where  $\lambda_1(X_0) > 0$ . Fig. 2.11(c) illustrates the fact the derivative of  $\lambda_1$  along  $\mathbf{v}_1$  vanishes.  $f(X, X_c) = -\frac{\partial s}{\partial X}|_{X_c} + s(X)$  is a flat function (at least up to the third order) along  $\mathbf{v}_1$  at  $X_c$ , i.e. the contours close to the value  $f(X_c)$  are at first approximation, ellipses whose larger axes are roughly parallel to  $\mathbf{v}_1(X_c)$  and with large ratios of the major axes length to the minor’s one.

In fig. 2.12 on page 32 the two criteria given in def. 6 are plotted for the van der Waals model. The thin line corresponds to  $\lambda_1 = 0$  and the thick one to  $\mathbf{v}_1 \cdot \nabla \lambda_1 = 0$ . These two lines cross each other at the already known critical point  $X_c = (\epsilon = \epsilon_c, v = v_c)$ . There is no other point in the parameter space  $(\epsilon, v)$  satisfying the conditions for a critical point given in def. 6.

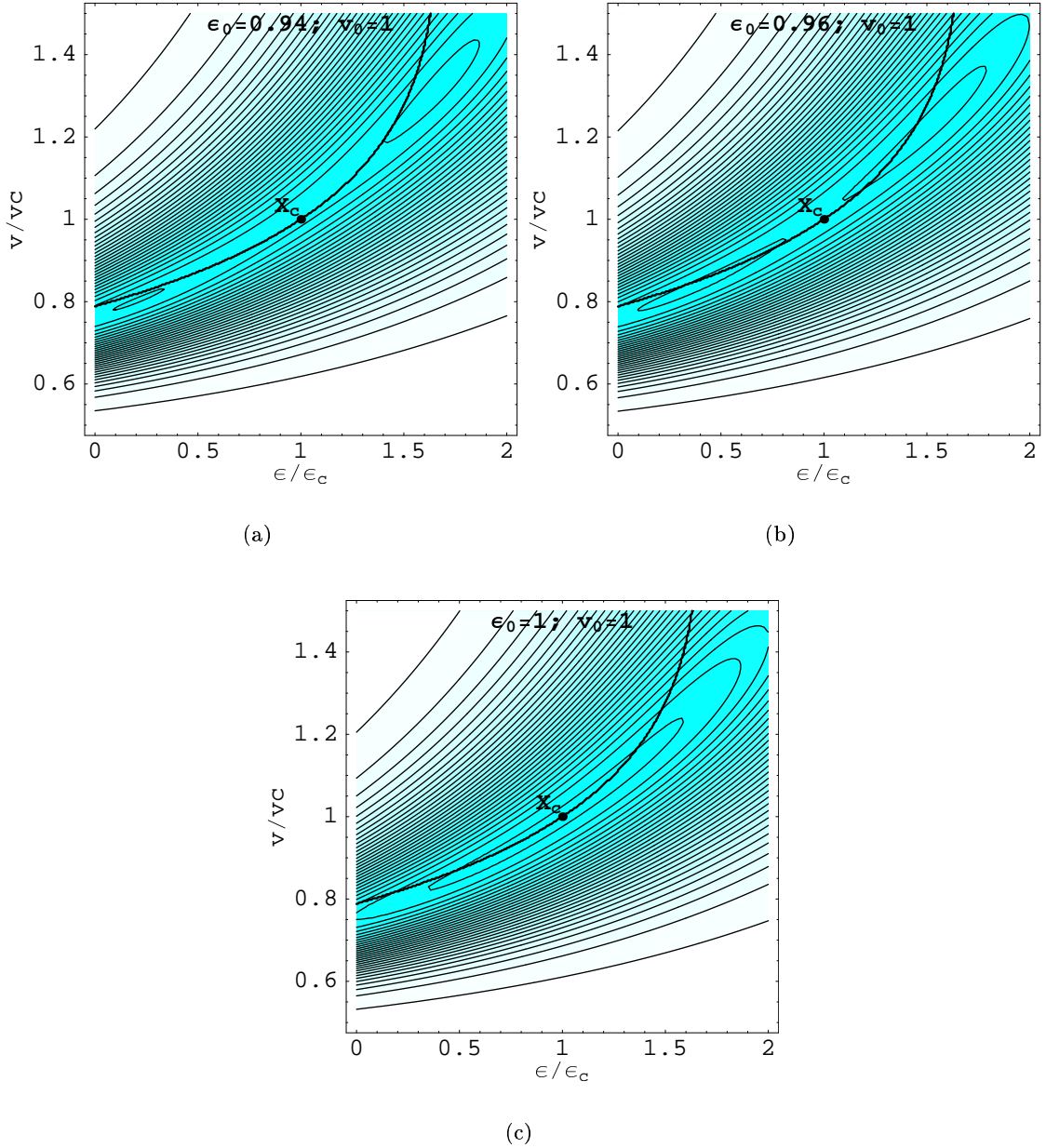


Figure 2.11: Contour density plot of  $f(\epsilon_0, v_0 = 1) = -x_0 \cdot X + s(X)$  for the vdW entropy-model, where  $x_0 = \frac{\partial S}{\partial X}|_{(\epsilon_0, v_0=1)}$  and for different values of  $\epsilon_0$ , when  $\epsilon_0 \rightarrow 1^-$ . The thick line locates  $\lambda_1 = 0$ . Below (above) this line  $\lambda_1$  is negative (positive). For  $v_0 = 1$  and  $\epsilon_0 < 1$ ,  $\lambda_1$  is positive.  $\lambda_1 > 0$  defines a first order phase transition region. There  $f$  ( $\sim$  minus the canonical free-energy) has two maxima in the pure phase regions (panels (a) and (b)). At the limit  $\epsilon_0 \rightarrow 1$ , these two maxima merge giving raise to a second order phase transition (see text).

## 2.4 Single event as a signal for phase transition?

Consider as an example, the study of the liquid-gas phase transition of metallic clusters (this transition is studied in part II). At very low energy all atoms are bounded in one

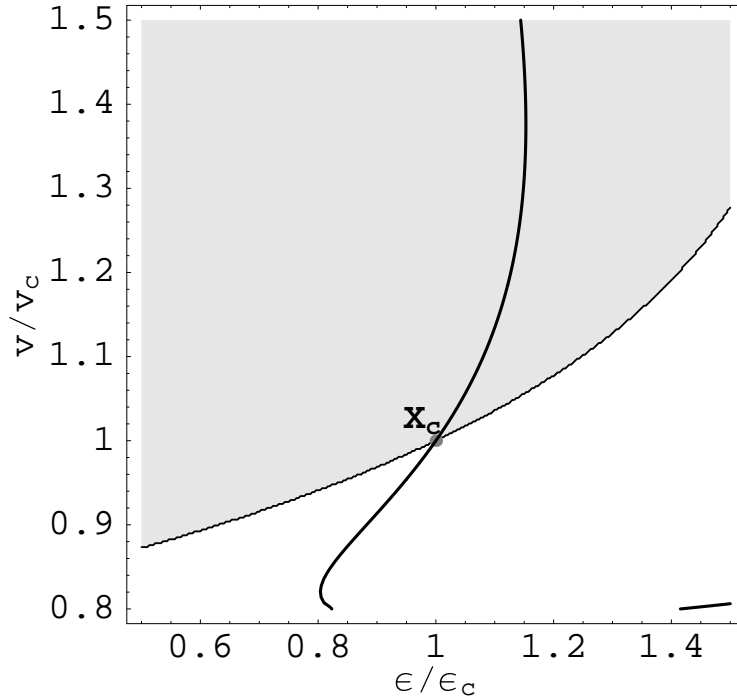


Figure 2.12: Criteria in def. 6 for second order phase transition applied to the vdW entropy-model. The thin and the thick lines correspond to  $\lambda_1 = 0$  and  $\mathbf{v}_1 \cdot \nabla \lambda_1 = 0$ , respectively. These two lines cross each other at the already known critical point at  $X_c = (\epsilon/\epsilon_c, v/v_c) = (1, 1)$  (gray dot). In the gray (white) region  $\lambda_1 > 0$  ( $< 0$ ).

big cluster (liquid phase). At higher energies the system enters the phase transition at an energy, say  $E = E_e$ , and starts to evaporate some monomers. Now, from a microcanonical experiment, where the energy  $E_1$  is fixed but *unknown*, an event is randomly singled out. Its mass distribution  $\mu_1$  is simply a big cluster and one monomer. The question is whether this event, characterized by  $\mu_1$ , signals the beginning (with increasing energy) of the phase transition. In other words, does  $\mu_1$  imply  $E_1 = E_e$ ?

As defined in the previous sections, phases and phase transitions are linked to the local properties of the microcanonical entropy surface. In its turn, the entropy is a property of an *ensemble* of states via Boltzmann's principle. Therefore, phases and phase transitions are properties of an *ensemble* of states and not of a *single* event.

Again, in other words, in a small system, a single event *cannot* be the signal of a phase transition. At most, one can single out from the ensemble an event that would characterize it by means of some most probable or average values of observables. E.g. at  $E = E_e$  events with  $\mu = \mu_1$  are the most probable ones. The inverse proposition is not necessarily true since the values of the observables can fluctuate (pretty much like the energy fluctuates in CE for small systems). For example, an ensemble may contain events with  $\mu_1$  though the energy of this ensemble is very different from  $E_e$ . Of course, in general, the probability for a single event to have  $\mu = \mu_1$  decreases as  $|E - E_e|$  increases. At the thermodynamical limit this probability becomes so small that the measurement of an event with  $\mu = \mu_1$  at  $E_1 \neq E_e$  may be regarded as practically impossible (to paraphrase Maxwell's own words [MAX]). Hence, at this limit the one-to-one mapping is recovered



$$\mu = \mu_1 \Leftrightarrow E = E_e.$$

## 2.5 Alternative theories

In this section two alternative frameworks for the thermostatics of small (or more generally non-extensive) systems are briefly reviewed. They are also compared with the theory presented in the previous sections. The first one tackles the problem of the lack of usual signals of phase transitions (Yang-Lee divergences) in CE by seeking their roots in the finite size partition function  $\mathcal{Z}$ . The other is based on an extension (generalization) of Boltzmann's principle by redefining the entropy  $S$ . Most of the introduction materials are taken directly from the respective literatures ([BMH00] for section 2.5.1 and [TSA99] for section 2.5.2).

### 2.5.1 Distribution of zeros

#### Classification of phase transitions

At the thermodynamical limit Lee and Yang [LY52A], Grossmann & al. [GL69] and Fisher [FIS65] showed that a classification of the phase transitions is made possible by studying the properties of the distribution of zeros (DOZ) of the partition function  $\mathcal{Z}(\mathcal{B})$  on the complex temperature plane ( $\mathcal{B} = \beta + i\tau$ ). The DOZ is on one (or many) dense line(s). This line crosses the real axis at the transition temperature and the angle made by this line with the real axis gives the order of the phase transition.

For finite size systems the DOZ is discrete and there is no zero on the real axis. The partition sum can be written as a function of its zeros  $\mathcal{B}_k = \mathcal{B}_{-k}^* = \beta_k + i\tau_k$  ( $k \in \mathbb{N}$ )

$$\begin{aligned} \mathcal{Z}(\mathcal{B}) &= \mathcal{Z}_{lim}(\beta) \mathcal{Z}_{int}(0) \exp(\mathcal{B} \partial_{\mathcal{B}} \mathcal{Z}_{int}(0)) \\ &\times \prod_{k \in \mathbb{N}} \left(1 - \frac{\mathcal{B}}{\mathcal{B}_k}\right) \left(1 - \frac{\mathcal{B}}{\mathcal{B}_k^*}\right) \exp\left(\frac{\mathcal{B}}{\mathcal{B}_k} + \frac{\mathcal{B}}{\mathcal{B}_k^*}\right) \end{aligned} \quad (2.8)$$

$$= \mathcal{Z}_{lim}(\beta) \prod_{k \in \mathbb{N}} \left(\frac{\tau_k^2 + (\beta_k - \mathcal{B})^2}{\beta_k^2 + \tau_k^2}\right) \exp\left(\frac{2\mathcal{B}\beta_k}{\beta_k^2 + \tau_k^2}\right) \quad (2.9)$$

where  $\mathcal{Z}_{lim}(\mathcal{B})$  describes the limiting behavior of  $\mathcal{Z}(\mathcal{B})$  for  $\mathcal{B} \rightarrow 0$  imposing

$$\lim_{\mathcal{B} \rightarrow 0} \mathcal{Z}_{int}(\mathcal{B}) = 1. \quad (2.10)$$

The free energy  $F(\mathcal{B}) = -\frac{1}{\mathcal{B}} \ln \mathcal{Z}(\mathcal{B})$ , has a derivative at every point in the complex temperature plane except at the zeros of  $\mathcal{Z}(\mathcal{B})$ . The calculation of the specific heat capacity  $C_V(\mathcal{B})$  by standard derivation yields

$$C_V(\mathcal{B}) = C_{Vlim}(\mathcal{B}) - \mathcal{B}^2 \sum_{k \in \mathbb{N}} \left(\frac{1}{(\mathcal{B}_k - \mathcal{B})^2} + \frac{1}{(\mathcal{B}_k^* - \mathcal{B})^2}\right). \quad (2.11)$$

Zeros of  $\mathcal{Z}(\mathcal{B})$  are poles of  $F(\mathcal{B})$  and  $C_V(\mathcal{B})$ . As can be seen from eq. (2.11) the major contributions to the specific heat capacity come from zeros close to the real axis, and a zero approaching the real axis infinitely close causes a divergence in the specific heat capacity.

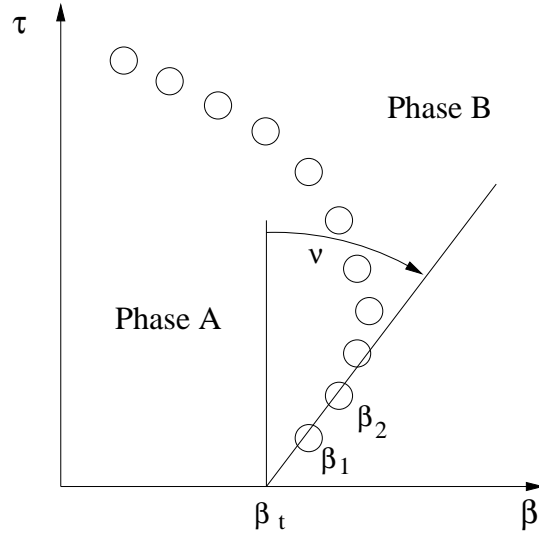


Figure 2.13: Schematic plot of the distribution of zeros on the complex temperature plane illustrating the definition of the classification parameters (taken from [MBHS00]). The circles give the positions of the zeros.

Borrmann et al. [BMH00, MBHS00, MB01] and Janke & Kenna [JK00] proposed a discretized version of Grossmann's classification scheme.

First let us assume that the DOZ lies approximately on a straight line near the real axis. The crossing angle of this line with the imaginary axis (see fig. 2.13) is then  $\nu = \tan \gamma$  with  $\gamma = (\beta_2 - \beta_1) / (\tau_2 - \tau_1)$ . The crossing point of this line with the real axis is given by  $\beta_t = \beta_1 - \gamma\tau_1$ . The discrete line density  $\phi$  as a function of  $\tau_k$  is defined as the average of the inverse distances between  $\mathcal{B}_k$  and its neighboring zeros

$$\phi(\tau_k) = \frac{1}{2} \left( \frac{1}{|\mathcal{B}_k - \mathcal{B}_{k-1}|} + \frac{1}{|\mathcal{B}_{k+1} - \mathcal{B}_k|} \right), \quad k = 2, 3, \dots \quad (2.12)$$

$\phi(\tau)$  in the region of small  $\tau$  is approximated by a simple power law  $\phi(\tau) \sim \tau^\alpha$ . A rough estimate of  $\alpha$  considering only the first two zeros gives

$$\alpha = \frac{\ln \phi(\tau_3) - \ln \phi(\tau_2)}{\ln \tau_3 - \ln \tau_2}. \quad (2.13)$$

When  $\alpha = 0$  and  $\gamma = 0$  the specific  $C_V$  exhibits a  $\delta$ -peak which corresponds to a first order phase transition. For  $0 < \alpha < 1$  and  $\gamma = 0$  or  $\gamma \neq 0$  the transition is of second order.

### Comments

All the previous discussion on the DOZ is made explicitly in the *canonical ensemble*. It is implicitly assumed that  $\mathcal{Z} < \infty$  (condition (0'), i.e.  $\mathcal{Z}$  converges) and that the distribution of the energy is well described by the canonical distribution. These points (in particular the latter one) are criticized for small systems in section 1.3 on page 11. See also [SSHT00, STH00] and part III where the studied system does not always fulfill condition (0').

The classification scheme based on the DOZ relies on the formally true fact that there is no information loss from ME to CE after the Laplace transform of  $\exp S$ . But in practice, the location of the zeros should be very sensitive to numerical precision leading to a loss of information [CH88]. The question whether and how information extracted from the DOZ is sensitive to these uncertainties deserve further studies. Moreover, the dimension of the parametric space to be explored as been multiplied by two. This complicates the classification for  $\mathcal{M} > 1$ . Furthermore, the richness of a system is reflected in the DOZ, see fig. 4(b) of [BMH00] where the classification is already difficult for small  $N \sim 30$ . An important question is how this complexity reflected in the DOZ affects the classification scheme and its usefulness. Finally, if the partition function cannot be estimated directly from analytical works, one has to Laplace transform the canonical probability distribution for different temperatures. This distribution is in its turn generally estimated by some numerical integration, e.g. Monte–Carlo integration. Here an important point is that one *cannot* use the usual optimization procedures to compute the probability distribution since there are only sensitive to extrema of  $P(X)$  leading to a tremendous loss of information. This information is needed to have an accurate DOZ. All in all, one must estimate  $P(X)$  over a broad  $X$ –range. But  $P(X)$  is nothing but the entropy  $S$  up to a linear constant which can be trivially removed. So, estimating  $P$  is also estimating  $S$  which contains already all the information about phases and phase transitions as shown in this chapter. Thus, in this respect, a classification based the local topology of  $S$  is more *direct* than the one using the DOZ.

## 2.5.2 Tsallis entropy

### Schematic overview

It is probably true that Boltzmann’s principle has its own domain of physical validity (much like classical mechanics is valid if at least the velocities involved are smaller than the speed of light). As an attempt to extent this yet hypothetical restricted domain Tsallis conjectured the following generalization of Boltzmann’s principle [TSA88]

$$S_q = k \frac{1 - \sum_{i=1}^W p_i^q}{q - 1}, \quad (2.14)$$

where  $\sum_{i=1}^W p_i = 1$ ,  $q \in \mathbb{R}$  and  $k^k$  is a positive constant and  $W$  is the total number of microscopic possibilities of the system. This expression recovers the usual Boltzmann–Gibbs entropy namely  $-k_B \sum_{i=1}^W p_i \ln p_i$  in the limit  $q \rightarrow 1$ . The entropic index  $q$  characterizes the degree of nonextensivity reflected in the following pseudo–additivity entropy rule

$$S_q(A + B) / k = S_q(A) / k + S_q(B) / k + (1 - q) (S_q(A) / k) (S_q(B) / k), \quad (2.15)$$

where  $A$  and  $B$  are two independent systems. Since  $S_q \geq 0$ ,  $q < 1$ ,  $q = 1$  and  $q > 1$  respectively correspond to superadditivity (superextensivity), additivity (extensivity) and subadditivity (subextensivity). The  $q$  expectation value  $\langle \mathcal{O} \rangle_q$  of an observable  $\mathcal{O}$  is

$$\langle \mathcal{O} \rangle_q = \frac{\sum_{i=1}^W p_i^q \mathcal{O}_i}{\sum_{i=1}^W p_i^q}. \quad (2.16)$$

---

<sup>k</sup> $k$  may also be a function of  $q$  provided that  $k \rightarrow k_B$  for  $q \rightarrow 1$  where  $k_B$  is Boltzmann’s constant [MNPP00, AMPP00].

Tsallis proved also in [TSA95] that the heat capacity

$$C_q \doteq T \frac{\partial S_q}{\partial T} = \frac{\partial U_q}{\partial T}, \quad (2.17)$$

is positive, i.e.

$$\frac{1}{q} C_q \geq 0, \quad (2.18)$$

$$q \frac{\partial^2 S_q}{\partial U_q^2} \leq 0. \quad (2.19)$$

### Comments

One of the main criticism found in the literature against Tsallis' entropy is the lack of physical interpretation for  $q$ . Its value is usually adjusted *a posteriori* in order to fit experimental data. For some authors,  $q$  is related to and determined by the microscopic dynamics [BLR, LBRT00], or to be more precise,  $q$  is linked to the system sensitivity to the initial conditions (see e.g. [AT98]). For others,  $q$  describes effects due to the finiteness of the heat bath. I.e. the heat bath heat capacity is not infinity as it is usual assumed to build the canonical distribution function, but instead  $C_v \propto (q - 1)^{-1}$  [ALM01]. The latter point illustrates how Tsallis' entropy (at least how it is used in literature) is closely related to the canonical ensemble. Even Tsallis is keen on keeping the Legendre structure of his theory, *imposing* therefore a positive heat capacity as shown in [TSA99, TSA95].

For the followers of Tsallis' entropy, the domains where Boltzmann's principle is no longer valid are e.g. long-range systems and those with (multi-)fractal boundary conditions [TSA99]. At least for long-range interaction systems, it is the *usual canonical description that appeared to be un-valid*, whereas up to now they could be well described within the *microcanonical ensemble* avoiding the need of an extension of Boltzmann principle (see part III, see also [GRO01, PAD90] and references quoted therein).

## 2.6 Conclusions

By studying the topology of the microcanonical entropy defined via Boltzmann's principle one can define phases and phase transitions for any physical system without invoking the thermodynamical limit.

The microcanonical ensemble is the proper ensemble for "small" systems. It gives a deeper insight onto the physical properties of "small" systems than *any* other "canonical" ensemble.

Up to now, the thermostatistics of small systems, as presented in this chapter, has been very successful [GRO01, GMS97, GRO90, DGC<sup>+</sup>00]. However, there are still open questions. E.g. is there a second law for "small" systems and how to express it without invoking the thermodynamical limit [GRO00A]? What are the links between the critical exponent in CE to the local topology of the microcanonical entropy-surface?

In the following, original studies of the equilibrium properties of two systems far from the thermodynamical limit are presented. In part II, the liquid-gas phase transition of small sodium clusters is explored as a function of the system size and also of the microcanonical pressure. On the other hand of the physical length scale, the equilibrium properties of a self-gravitating system at fixed total energy and angular momentum are studied in part III.